Quantification of the Therapeutic Response of Intraretinal, Subretinal, and Subpigment Epithelial Compartments in Exudative AMD during Anti-VEGF Therapy

Isabelle Golbaz, Christian Ahlers, Geraldine Stock, Christopher Schütze, Sabine Schriefl, Ferdinand Schlanitz, Christian Simader, Christian Prünte, and Ursula Margarethe Schmidt-Erfurth

Purpose. To analyze the functional and morphologic effects of different ranibizumab treatment regimens on retinal and subretinal as well as sub-RPE compartments in neovascular age-related macular degeneration (nAMD) using spectral-domain optical coherence tomography (SD-OCT) and manual segmentation software.

Methods. Twenty-seven eyes of 27 patients with nAMD were examined over a 12-month period. Two treatment arms received either monthly or quarterly administered intravitreal ranibizumab. Intraretinal, subretinal, and sub-RPE volume equivalents were delineated using manual segmentation software over a defined series of B-scans obtained by SD-OCT. The mean area in pixels was calculated for each compartment at each time interval.

Results. SD-OCT and manual segmentation allowed for exact identification of intraretinal, subretinal and sub-RPE compartments and their responses to different treatment regimens. The loading dose demonstrated a corresponding treatment effect on all anatomic parameters. In contrast to the sub-RPE compartment, intraretinal fluid accumulation and subretinal fluid accumulation (SRFA) demonstrated an immediate response to ranibizumab therapy. The overall plasticity of the morphologic response declined over time. In general, SRFA demonstrated greater sensitivity for therapeutic effects and was more frequently associated with recurrent disease.

Conclusions. An exact quantification of fluid in different anatomic compartments based on SD-OCT imaging, using appropriate segmentation software systems, may be useful to determine optimal treatment and retreatment parameters and explains the lack of correlation of best-corrected visual acuity and conventional OCT values. (*Invest Ophthalmol Vis Sci.* 2011;52:1599–1605) DOI:10.1167/iovs.09-5018

Age-related macular degeneration (AMD) is one of the leading causes of legal blindness in patients older than 60 years. Finding effective treatment strategies is therefore of high socioeconomic interest.[1] In addition to the known age dependency of the disease, complex interactions among metabolic, environmental, and genetic factors seem to induce changes, chronically alternating retinal and subretinal structures in the central retina. These pathophysiologic stimuli contribute to the varying appearance of AMD over a wide spectrum of dry and exudative changes. Improvements in the development of adequate therapeutic strategies inhibiting vascular endothelial growth factor (VEGF) offer a distinguished progress in the management and have improved the prognosis of neovascular AMD (nAMD). Intravitreally applied antiangiogenic substances are able to resolve intraretinal and subretinal edema restoring the physiological morphology of the macula and consecutively also visual function. The efficacy of anti-VEGF substances (e.g., ranibizumab) has been demonstrated in multiple clinical trials. Particularly, repeated intravitreal injections of ranibizumab in monthly intervals during the first 3 months of therapy have demonstrated a positive anatomic and functional impact regarding visual acuity and reduction of leakage in fluorescein angiography (FA).[2] Therefore, a so-called loading phase consistent with three initial injections was included in the official recommendations for ranibizumab therapy by the Food and Drug Administration (FDA) for the United States and the European Medicines Agency for European countries.[3] During this initial loading interval, the most intensive morphologic and functional changes are documented under therapy, suggesting this phase for detailed analysis of anatomic, functional response patterns.[2]

To evaluate the long-term effects, most studies of anti-VEGF treatment extend over a 24-month period. Noteworthy, these trials suggest a strict monthly treatment regimen. Although functional parameters and morphologic changes were documented using ETDRS visual acuity testing, optical coherence tomography (OCT), biomicroscopy, and FA, none of these parameters were allowed to guide treatment decisions in the approval studies (ANCHOR, MARINA). Interestingly, some investigator-driven studies implemented individual flexible regimens based on OCT findings.[4–7]

Meanwhile, OCT has become the most valuable noninvasive retinal imaging modality enabling for differentiation of intraretinal layers and different compartments.[8] The development of spectral domain OCT (SD-OCT) has further enlarged the clinical applicability of OCT imaging. Discrete structures such as the external limiting membrane (ELM) and the photoreceptor inner/outer cone segments (IS/OS) can be imaged in detail.[9–12] More advanced analyses of SD-OCT data offer novel perspectives in diagnosis and follow-up monitoring of nAMD. Taking advantage of the high scanning speed of SD devices, a

From the Department of Ophthalmology, Medical University of Vienna, Vienna, Austria.

Submitted for publication December 4, 2009; revised April 6 and August 7, 2010; accepted September 1, 2010.

Disclosure: **I. Golbaz**, None; **C. Ahlers**, None; **G. Stock**, None; **C. Schütze**, None; **S. Schriefl**, None; **F. Schlanitz**, None; **C. Simader**, None; **C. Prünte**, None; **U. Schmidt-Erfurth**, None

Corresponding author: Ursula Schmidt-Erfurth, Medical University Vienna, Department of Ophthalmology, Waehringer Guertel 18-20, A-1090 Vienna, Austria; ursula.schmidt-erfurth@meduniwien.ac.at.

Copyright 2011 The Association for Research in Vision and Ophthalmology, Inc.

Downloaded from iovs.arvojournals.org on 04/23/2021

dense raster scanning at all locations of the central retina is obtained, allowing for a delineation of complete compartments with intraretinal and subretinal locations. A more detailed assessment of the morphologic effects of anti-VEGF therapy on defined retinal and subretinal compartments and subsequently a quantification of fluid volumes may allow identifying realistic parameters relevant for optimizing therapeutic strategies and improved evaluation of disease progression and prognosis.

It was the aim of this study to evaluate characteristic morphologic changes in the three anatomic compartments—intraretinal, subretinal, and subpigment epithelial—in patients with nAMD receiving anti-VEGF therapy, using an SD-OCT system and manual segmentation software approved by the FDA. This segmentation technique avoids algorithm-based artifacts in the delineation of retinal structures, which have been reported to occur frequently in nAMD.[13–15] Accurate measurements of changes in specific retinal compartments were performed, analyzed over a 12-month period, and correlated with functional parameters.

Patients and Methods

Patients' Inclusion Criteria and Treatment

Twenty-seven eyes of 27 patients with new-onset nAMD were examined. All patients presented exudative changes in at least 1 of 3 retinal and subretinal compartments. A standardized ophthalmologic examination—including best-corrected visual acuity (BCVA), FA (HRA2; Heidelberg Engineering, Heidelberg, Germany), conventional OCT, and SD-OCT—were performed.

Inclusion criteria were defined as visual acuity (VA) ranging from 20/40 to 20/320 and a total lesion size of <9 disc areas, with the CNV covering >50% of the total lesion size. Patients had to be older than 50 years of age.

Patients were excluded from the study if they had received previous treatment with antiangiogenic drugs, photodynamic therapy, or intravitreal corticosteroids. Further exclusion criteria were any surgical procedure carried out within the last 6 months before inclusion, postvitrectomy status, and current aphakia.

Written informed consent after extensive discussion on the benefits and possible risks of treatment and examination procedures was obtained from each patient. The institutional ethics committee approved the study procedures, including therapeutic and diagnostic examinations. The protocol complied with the tenets of the Declaration of Helsinki. All examinations were performed at the Department of Ophthalmology, Medical University Vienna, Austria.

Antiangiogenic Treatment and Patient Follow-up

The study represents an ancillary study to the EXCITE trial focusing an analysis of SD-OCT imaging (U. Schmidt-Erfurth, et al., on behalf of the EXCITE Study Group, unpublished data, 2009). A screening visit was performed within 10 days before the initial intravitreal injection with ranibizumab was carried out. BCVA, OCT, and SD-OCT examinations were performed at all monthly visits following a standardized protocol. FA was scheduled at baseline, week 12, and week 52. Patients were randomly assigned to three different regimens to assess the differential effect of treatments applied in the quarterly or monthly regimen.

All patients obtained an identical loading regimen of three consecutive monthly injections with intravitreal ranibizumab. The drug dose differed among the different treatment arms. The first treatment group received three monthly injections of 0.3 mg ranibizumab followed by injections given every third month, whereas the second treatment group received 0.5 mg ranibizumab after the same regimen. The third group received 0.3 mg ranibizumab in monthly intervals.

Given that no significant differences could be found in the outcome parameters between the two dose groups receiving similar quarterly doses (U. Schmidt-Erfurth, et al., on behalf of the EXCITE Study Group, unpublished data, 2009), these two groups were merged into a single quarterly treatment group for analysis. All patients were masked to their group affiliation and received a sham injection at treatment-free visits according to the protocol of the EXCITE trial.

Data Acquisition and Software Analysis

Spectral Domain Optical Coherence Tomography. Three-dimensional (3D) imaging of the macular region was performed using a commercially available SD-OCT system (Cirrus; Carl Zeiss Meditec, Dublin, CA). The device has an axial resolution of 6 μm and a maximum scanning speed of 25,000 A-scans/s. The scanned area used for quantitative analysis of different compartments had a dimension of 6×6 mm. A $512 \times 128 \times 1024$ macular raster mode was selected for manual segmentation and compartment analysis.

Manual Segmentation. Manual segmentation and volumetric analysis were performed using imaging software (3D-Doctor; Able Software Corp., Irvine, CA) approved by the FDA for medical imaging and 3D visualization. This software has previously been used in scientific publications and offers the opportunity to generate 3D models of different compartments.[7,16,17] Certified graders of the Vienna Reading Center (VRC; Department of Ophthalmology, Medical University Vienna) performed manual segmentations in a defined set of 11 of 128 B-scans of a complete macular raster scan. This selection was gathered as manual segmentation in a time-consuming process. The following scans were defined as representative and segmented in every individual raster scan: numbers 24, 34, 44, 54, 59, 64, 69, 74, 84, 94, and 104.

An appropriate representativeness of exudative changes of the entire macular region was assumed after a comprehensive screening of the extension of fluid pooling in the study population (Fig. 1a) because these 11 scans included five central, four pericentric, and two peripheral scans. Each grader had undergone a thorough certification process in OCT grading at the VRC before approval to grade study images was given. Retinal parameters analyzed in this study consisted of the retinal area (IRFA), including the intraretinal space between the inner limiting membrane (ILM) and the IS/OS barrier, the area of the subretinal fluid accumulation (SRFA) extending from the IS/OS barrier and the RPE layer, and the area of the pigment epithelial detachment (PEDA; Fig. 1b). Imaging software (3D-Doctor; Able Software Corp.) measured the different areas (IRFA, SRFA, PEDA) in pixels for each scan and summed up the results of the scans for each patient per visit (Fig. 1c). Areal measurements were performed for the single scans. However, we decided not to present volumetric calculations because the scan selection made for quantitative analysis in this study likely introduced lateral distortion, and thereby systemic bias, into the results.

Because of the time-consuming nature of manual segmentation analysis, we were unable to perform the analysis in an isodense manner throughout the scanned area. Interpolation of the data from the scans chosen would consecutively result in an overestimation or underestimation of changes in the central, perifoveal, and parafoveal regions.[18] Improved automatic segmentation procedures will hopefully be able to bridge this gap in the near future; analysis of complete raster scans was not possible for us applying the manual segmentation techniques limited to this number of patients and follow-up visits.

We performed masked quality control measurements on a sample of images. Therefore, two graders analyzed the measurements of five patients before and after VEGF treatment (Fig. 1d).

Visual Acuity. BCVA was measured monthly according to a standardized refraction procedure using ETDRS charts at 2 meters and 4 meters.

Statistical Analysis

For evaluation and documentation of masked patient data, a commercial database (Excel; Microsoft, Redmond, WA) was used. Statistical analyses were performed (SPSS for Windows, version 12.0; SPSS, Chicago, IL). $P < 0.05$ was considered statistically significant.

Downloaded from iovs.arvojournals.org on 04/23/2021

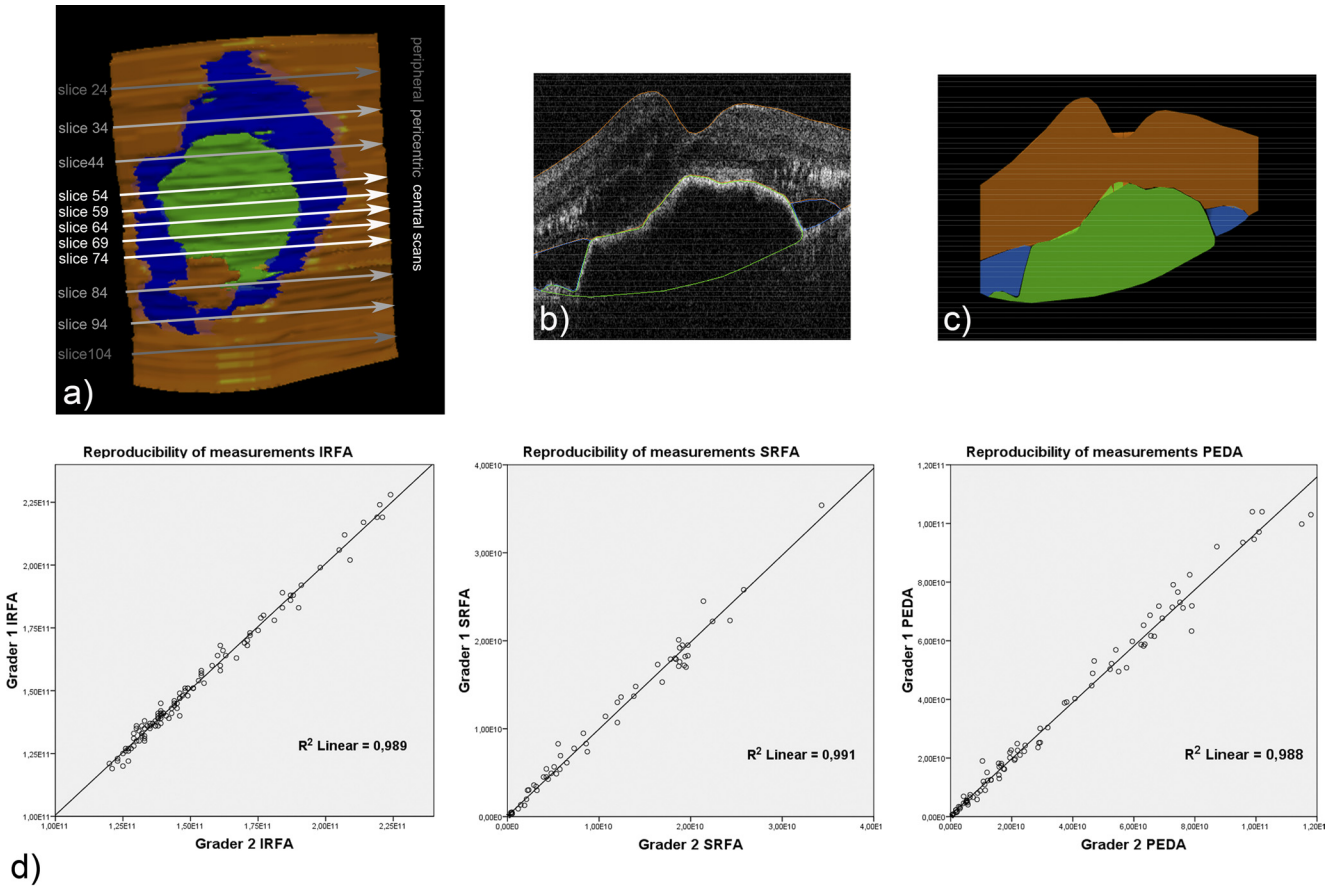

FIGURE 1. Manual segmentation. (**a**) Localization of 11 of 128 B-scans selected for analysis in this study. (**b**) Accurate identification of the three different compartments was carried out by manual segmentation of each selected B-scan. *Orange line*: delineation of the intraretinal space between the ILM and IS/OS barrier (IRFA). *Blue line*: area of the subretinal fluid extending from the outer retina and the RPE layer. *Green line*: PEDA. (**c**) 2D slice of a segmented B-scan. IRFA (*orange*), SRFA (*blue*), and PEDA (*green*) were visualized. (**d**) Masked quality control of measurements of the three different compartments of five data sets before and after treatment, performed by two graders (IRFA, $R^2 = 0.989$; SRFA, $R^2 = 0.991$; PEDA, $R^2 = 0.998$).

RESULTS

Visualization of Retinal Compartments

Three defined compartments of the macular region were delineated, and their anatomic extension was quantified in this study (IRFA, SRFA, and PEDA) to document the impact of different treatment regimens on the macular morphology. The intensity and time course of the therapeutic response was followed over 12 months and correlated individually with visual acuity. Group A received monthly injections, and group B was treated at quarterly intervals after a loading regimen.

BCVA in Different Dosing Regimens

All patients received a loading dose containing three monthly injections of ranibizumab. The mean improvement in BCVA at month 3 was +7.4 letters.

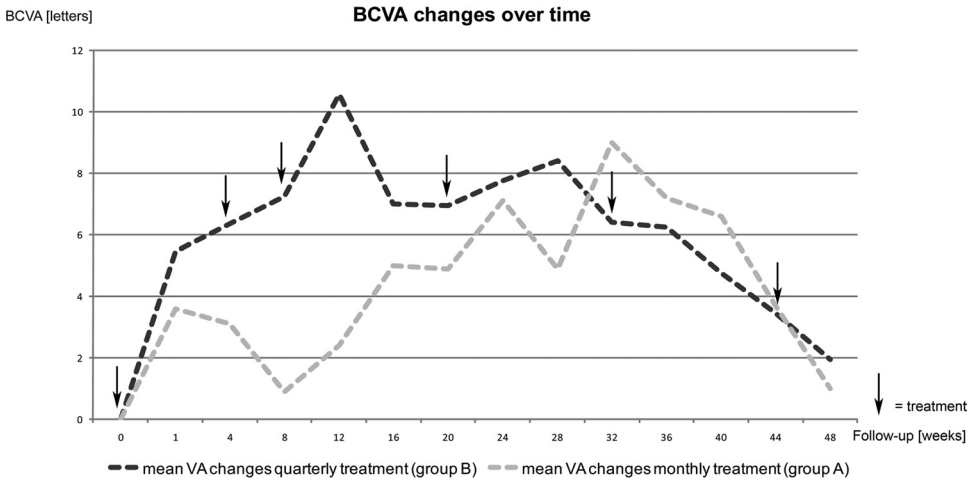

FIGURE 2. BCVA changes over time. This diagram shows the time course of BCVA for both treatment arms. Group A, monthly treated group; group B, quarterly injection group. Both groups received a loading dose of three monthly injections of ranibizumab within the first 3 months.

Downloaded from iovs.arvojournals.org on 04/23/2021

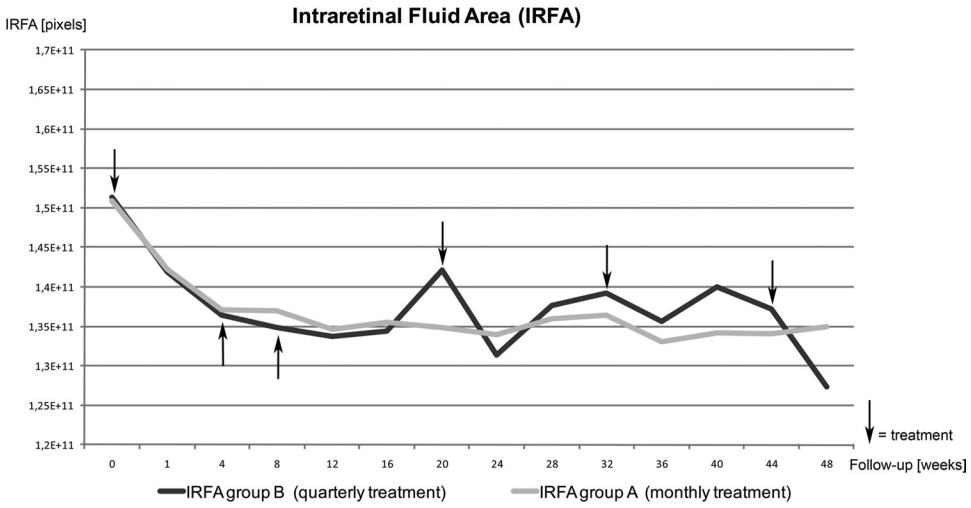

FIGURE 3. Changes of the IRFA. Specific response of the IRFA in both groups. Significant decrease ($P < 0.04$) of intraretinal edema could be identified during the loading dose in both groups. Group B showed a recurrent increase of IRFA in each treatment-free period, whereas group A demonstrated continuously low IRFA values during the entire follow-up.

No overall improvement could be shown for BCVA between baseline and month 12 in group A (+1 ± 13.6 letters; Fig. 2). Interestingly, the group receiving quarterly treatment (Fig. 2) showed a fluctuating "spike and wave" effect in BCVA. The mean change in BCVA in group B was +1.9 ± 9.6 letters at month 12.

An improvement in BCVA was apparent after each drug application but was regularly lost at the end of the treatment-free 3-month interval. Despite further treatment, group A and group B showed continuous deterioration in BCVA with a loss in the therapeutic benefit after month 8. Notably, BCVA of the quarterly treatment group B rose sharply during the loading phase but did never recover to this level during the following treatment periods. Best VA outcomes were uniformly evident during the initial period of anti-VEGF treatment (Fig. 2).

Specific Responses of Different Compartments

Intraretinal Fluid. Manual segmentation of mean IRFA revealed a significant decrease ($P < 0.04$) of intraretinal edema during the first three injections and could be identified in both groups (Fig. 3).

In the absence of further continuous treatment, IRFA showed a recurrent increase in each treatment-free period of 8 weeks in the quarterly treated groups. This increase of intraretinal area was significant ($P > 0.03$) and immediately resolved after the subsequent intravitreal injection (Fig. 3). IRFA did not reach the lowest value achieved after the loading dose during the following 6 months. Interestingly, IRFA significantly decreased below loading dose values at the end of the study after quarterly treatment had been applied for at least 10 months after the initiation of treatment.

Group A demonstrated a rapid decline in IRFA followed by continuously low IRFA values during the entire follow-up period (Fig. 3). Comparison of BCVA with intraretinal changes showed a negative correlation between BCVA and IRFA during follow-up (Fig. 4).

Subretinal Fluid. Both groups showed a rapid resolution of SRF during the loading dose. Group B, which received quarterly treatment, demonstrated a prompt recurrence of SRF during each treatment-free phase. The rapid and repetitive recurrence of SRF followed an identical pattern in intensity and time course independent of the follow-up duration.

Group A presented consistently low values of SRF with an absence of recurrence for most of the follow-up period; mild reaccumulation was noted during the last visits before month 12 (Fig. 5). Interestingly, the reappearance of SRF was more intensive than the recurrence of IRFA in all groups in terms of absolute values (pixel area), indicating that SRF responds most sensitively to the type of treatment regimen and showing an immediate increase in SRFA with treatment discontinuation and an equally rapid resolution subsequent to antiangiogenic intervention.

Comparing the course of SRFA extension and BCVA in the quarterly treated group B, a clear negative correlation was

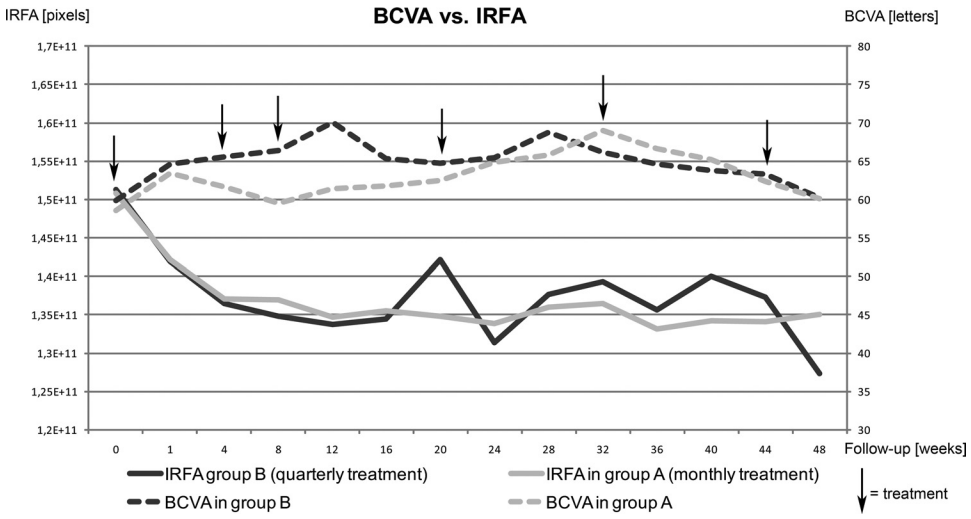

FIGURE 4. Comparison of BCVA with IRFA changes showed a negative correlation between these parameters during follow-up.

Downloaded from iovs.arvojournals.org on 04/23/2021

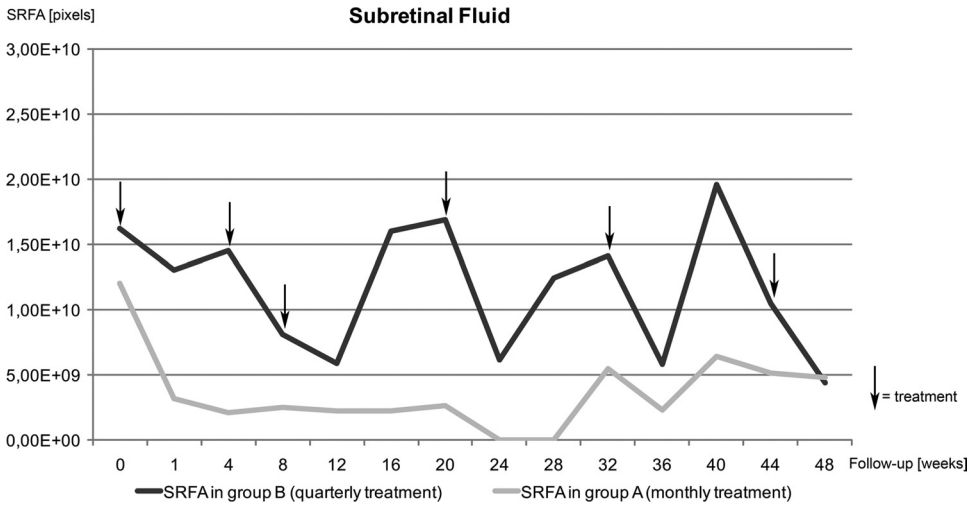

FIGURE 5. Specific response of SRFA to anti–VEGF therapy. Both groups showed a rapid resolution of SRFA during the loading dose. Group B demonstrated prompt recurrence of SRF during each treatment-free phase. Group A presented consistently low values of SRFA.

identified during the loading dose ($P < 0.05$). BCVA increased rapidly during resolution of SRFA in the early treatment phase. This inverse effect was maintained during follow-up with quarterly interventions, though in a less accentuated manner during late follow-up (Fig. 6a).

Group A, which underwent continuous monthly therapy, also revealed a resolution of SRF and a concomitant increase in BCVA at the beginning of the study and during most of the maintenance phase. However, during the last intervals, BCVA consistently decreased and SRFA irregularly increased (Fig. 6b).

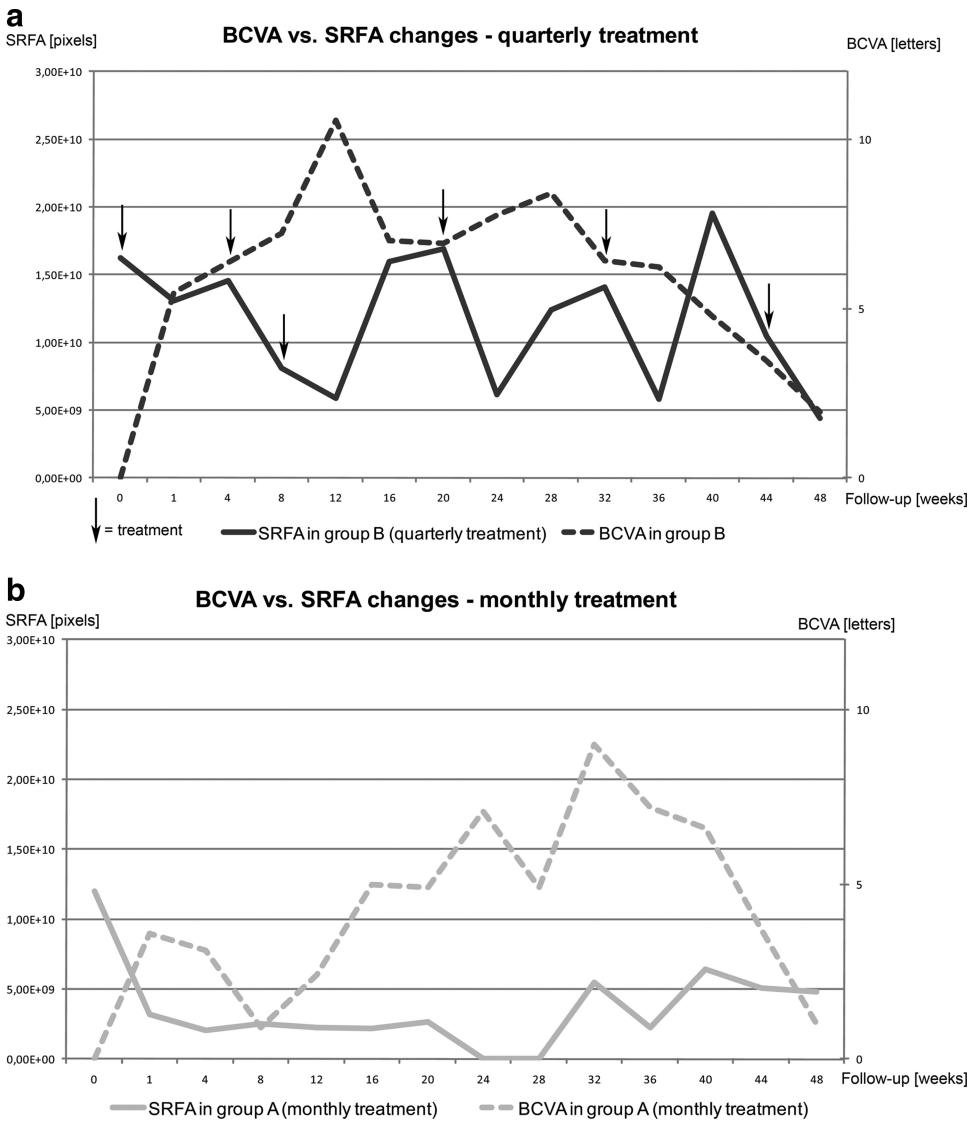

FIGURE 6. (**a**) Comparison of BCVA with SRFA changes in group B. A clear negative correlation was found ($P < 0.05$) during the loading dose. This inverse could also be observed during follow-up. (**b**) Comparison of BCVA with SRFA changes in group A. Group A presented a resolution of SRFA and a concomitant increase in BCVA during the loading dose and during the maintenance phase. An irregular increase of SRFA and a decrease in BCVA in the last months of the study can be observed.

Downloaded from iovs.arvojournals.org on 04/23/2021

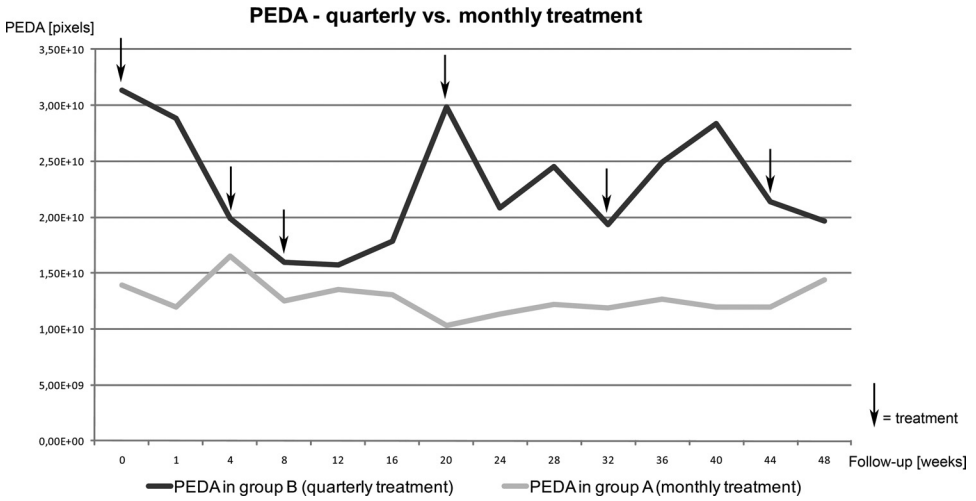

Figure 7. Specific response of PEDA to anti–VEGF therapy. Group B showed no significant response of PEDA to anti-angiogenic therapy. Group A presented a maintained reduction in PEDA.

Pigment Epithelial Detachment

Fluid under PEDA showed no significant positive response to therapy in group B (receiving quarterly injection). In contrast, a maintained reduction in PEDA ($P < 0.04$) could be identified in group A (Fig. 7). No correlation between BCVA and the behavior of the sub-PED fluid area was identified in either group (Fig. 8).

Discussion

This study was performed to evaluate the effects of intravitreal ranibizumab therapy on the three "classical" morphologic compartments of the central macular anatomy in eyes with AMD. The intraretinal, subretinal, and sub-RPE compartments were analyzed over a 12-month period. Certified graders performed manual segmentation and accurate delineation of the photoreceptor OS and the RPE layer in 11 representative B-scans per visit. This procedure of collecting multiple areas of fluid accumulation per compartment was chosen to ascertain that a realistic quantification of the entire fluid pooling at each visit was obtained independently of random localization of a single scan through any topography of the exudative lesion. SD-OCT imaging was used, and individual segmentation was performed to obtain accurate values and, at the same time, to avoid misleading information due to the false segmentation that occurs frequently in automatic analysis of retinal morphology.[13]

The time course of the response of the individual compartments was plotted and correlated with BCVA to identify the most clinically relevant parameters. Two treatment regimens were applied—one group underwent quarterly intermittent intervention and one group underwent continuous monthly treatment.

During the loading phase, both groups showed similarly significant improvement in BCVA. However, this therapeutic benefit could not be maintained during extended follow-up in either group. Such a loss in functional gain is common with a quarterly regimen but is also within the expected limits with monthly retreatments in a relatively small study population of 27 patients, particularly in a selection group with massive exudative changes in all three compartments. The quarterly regimen group and the monthly regimen group reflected the efficacy of ranibizumab with significant thinning of the IFRA. Between 4 and 11 months, however, IRFA values in the quarterly treated group were of higher consistency than in the monthly regimen group. Interestingly, a significant reduction in IRFA below loading dose values could be observed at month 12 ($P < 0.02$) after a ranibizumab dose at month 11, indicating that the neurosensory retina might have been subject to significant atrophy during the preceding year of discontinuous treatment. In general, a decrease of IRFA values consistent with intraretinal edema was associated with an improvement in visual function, at least over the first 9 months of follow-up.

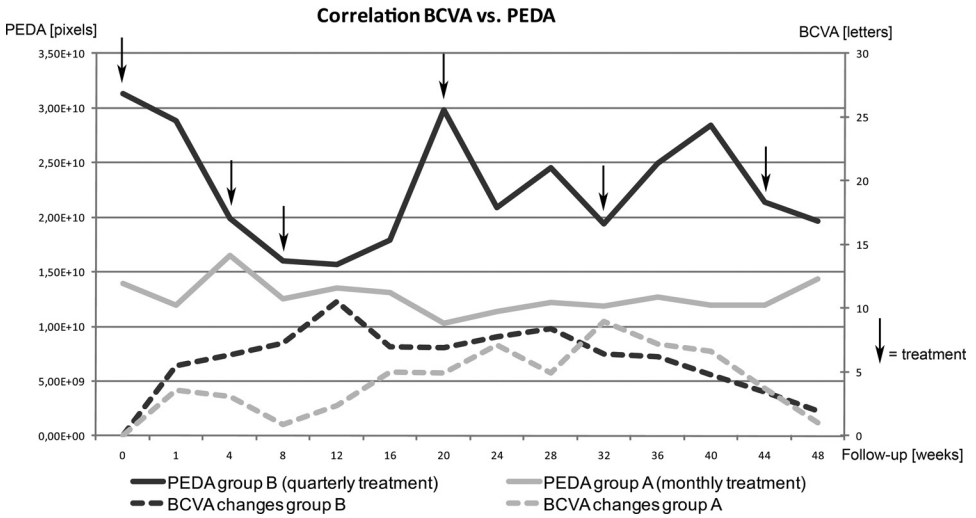

Figure 8. Comparison of BCVA with PEDA changes in both groups.

Downloaded from iovs.arvojournals.org on 04/23/2021

Fluctuations in central retinal thickness or IRFA were induced by the quarterly regimen but were only moderate and were not associated with fluctuations in BCVA values. Segmentation of SRFA highlighted an immediate and accentuated response to intravitreal ranibizumab during the initial injections of the loading phase. Earlier publications have already discussed the important role of subretinal fluid for visual function.[7,17]

More detailed and robust data of this study showed that recurrence of disease, which could regularly be observed in the quarterly regimen, is predominantly reflected in the response of SRFA rather than of IRFA. With each discontinuation of intravitreal therapy, SRFA values showed an immediate and pronounced response. More important, the morphologic change was translated in an identical pattern of BCVA fluctuations in a direct correlation of timing and intensity. Interestingly, the loss of vision during the last follow-up visits in the monthly regimen also appeared to be correlated with a rebound effect at the level of the SRFA. OCT manufacturers are, therefore, encouraged to develop segmentation algorithms able to identify SRF precisely because SRF may clearly be a more sensitive and clinically relevant parameter to guide treatment regimens than retinal thickness, if assessed correctly.

With this insight, it is not surprising that no correlation between visual acuity and central retinal thickness can be found as long as the accumulation of subretinal fluid and intraretinal fluid is not differentiated and SRF is not measured. Although the initial decrease in SRFA was directly associated with an improvement in BCVA, this association became less evident during follow-up. With under-treatment in the quarterly regimen, photoreceptor damage might have become irreversible. Recurrent SRF induces a loss in the functional plasticity of retinal tissue over time. Progressive neurosensory atrophy is another reason for a lack of correlation in BCVA and conventional central retinal thickness values over time.

Finally, our analysis demonstrated a reduction of PEDA during the loading dose. However, this initial effect could not be observed during further follow-up. This finding is in concordance with other studies showing neither a qualitative nor a quantitative effect of anti-VEGF therapy on PEDA amount. Furthermore, this study found no correlation between PEDA anatomy and visual function as reported by other authors in phase 3 clinical trials.[19]

Precise knowledge of the changes in different macular compartments with respect to visual acuity and time course of recurrence is essential to identify optimal parameters to guide treatment. Given that automatic segmentation analyses are strongly compromised by a significant amount of errors, a manual approach was chosen to avoid these technological limitations in this study. However, manual segmentation is time-consuming and is, therefore, not applicable in clinical practice. Advanced automated procedures are needed to identify relevant features rapidly and reproducibly in the future.

In conclusion, meticulous analysis of intraretinal, subretinal, and sub-RPE compartments will enable better understanding of antiangiogenic therapy in neovascular AMD. SRFA has been demonstrated as the most relevant morphologic parameter, indicating disease recurrence and efficacy of anti–VEGF intervention.

Acknowledgments

The authors thank the patients who participated in the study, the certified graders of the Vienna Reading Center, and Ursula Heiling, Judith Pulgram, and Andreas Nahrgang for technical assistance.

References

1. Shah AR, Del Priore LV. Natural history of predominantly classic, minimally classic, and occult subgroups in exudative age-related macular degeneration. *Ophthalmology.* 2009;116:1901–1907.
2. Bolz M, Simader C, Ritter M, et al. Morphological and functional analysis of the loading regimen with intravitreal ranibizumab in neovascular AMD. *Br J Ophthalmol.* 2010;94:185–189.
3. Kaiser PK, Blodi BA, Shapiro H, Acharya NR. Angiographic and optical coherence tomographic results of the MARINA study of ranibizumab in neovascular age-related macular degeneration. *Ophthalmology.* 2007;114:1868–1875.
4. Fung AE, Lalwani GA, Rosenfeld PJ, et al. An optical coherence tomography-guided, variable dosing regimen with intravitreal ranibizumab (Lucentis) for neovascular age-related macular degeneration. *Am J Ophthalmol.* 2007;143:566–583.
5. Lalwani GA, Rosenfeld PJ, Fung AE, et al. A variable-dosing regimen with intravitreal ranibizumab for neovascular age-related macular degeneration: year 2 of the PrONTO Study. *Am J Ophthalmol.* 2009;148:43–58, e41.
6. Cohen SY, Dubois L, Tadayoni R, et al. Results of one-year's treatment with ranibizumab for exudative age-related macular degeneration in a clinical setting. *Am J Ophthalmol.* 2009;148:409–413.
7. Ahlers C, Golbaz I, Stock G, et al. Time course of morphologic effects on different retinal compartments after ranibizumab therapy in age-related macular degeneration. *Ophthalmology.* 2008; 115:e39–e46.
8. Drexler W, Fujimoto JG. State-of-the-art retinal optical coherence tomography. *Prog Retin Eye Res.* 2008;27:45–88.
9. Pieroni CG, Witkin AJ, Ko TH, et al. Ultrahigh resolution optical coherence tomography in non-exudative age related macular degeneration. *Br J Ophthalmol.* 2006;90:191–197.
10. Schmidt-Erfurth U, Leitgeb RA, Michels S, et al. Three-dimensional ultrahigh-resolution optical coherence tomography of macular diseases. *Invest Ophthalmol Vis Sci.* 2005;46:3393–3402.
11. Hee MR, Baumal CR, Puliafito CA, et al. Optical coherence tomography of age-related macular degeneration and choroidal neovascularization. *Ophthalmology.* 1996;103:1260–1270.
12. Srinivasan VJ, Wojtkowski M, Witkin AJ, et al. High-definition and 3-dimensional imaging of macular pathologies with high-speed ultrahigh-resolution optical coherence tomography. *Ophthalmology.* 2006;113:2054 e2051–2014.
13. Sadda SR, Wu Z, Walsh AC, et al. Errors in retinal thickness measurements obtained by optical coherence tomography. *Ophthalmology.* 2006;113:285–293.
14. Leung CK, Chan WM, Chong KK, et al. Alignment artifacts in optical coherence tomography analyzed images. *Ophthalmology.* 2007;114:263–270.
15. Costa RA, Calucci D, Skaf M, et al. Optical coherence tomography 3: automatic delineation of the outer neural retinal boundary and its influence on retinal thickness measurements. *Invest Ophthalmol Vis Sci.* 2004;45:2399–2406.
16. Golbaz I, Ahlers C, Goesseringer N, et al. Automatic and manual segmentation of healthy retinas using high-definition optical coherence tomography. *Acta Ophthalmol.* In press.
17. Ahlers C, Golbaz I, Einwallner E, et al. Identification of optical density ratios in subretinal fluid as a clinically relevant biomarker in exudative macular disease. *Invest Ophthalmol Vis Sci.* 2009;50: 3417–3424.
18. Sadda SR, Keane PA, Ouyang Y, Updike JF, Walsh AC. Impact of scanning density on measurements from spectral domain optical coherence tomography. *Invest Ophthalmol Vis Sci.* 2010;51: 1071–1078.
19. Ritter M, Bolz M, Sacu S, et al. Effect of intravitreal ranibizumab in avascular pigment epithelial detachment. *Eye (Lond).* 2010;24: 962–968.

Downloaded from iovs.arvojournals.org on 04/23/2021